



Influence of Morpholinium-Based Ionic Liquid on the Aggregation Behavior of Cationic Surfactant and Imidazolium-Based Ionic Liquid with the same Alkyl Chain in an Aqueous Medium

Gagandeep Kaur¹ · Ramanjeet Kaur¹ · Jasmeet Kaur¹ · Subhra Yadav¹ · Harsh Kumar¹ · Pooja Sharma¹

Received: 28 February 2023 / Accepted: 20 May 2023 / Published online: 3 July 2023
© The Author(s), under exclusive licence to Springer Science+Business Media, LLC, part of Springer Nature 2023

Abstract

The purpose of this study is to investigate the influence of a morpholinium-based ionic liquid, *N*-pentadecyl-*N*-methylmorpholinium bromide [Mor_{1,15}]Br on the aggregation behavior of a conventional cationic surfactant, tetradecyltrimethylammonium bromide, and imidazolium-based surface-active ionic liquid, 1-tetradecyl-3-methylimidazolium bromide [C₁₄mim]Br in the aqueous medium. The aggregation behavior has been investigated in (0.00, 0.03, 0.06, and 0.10) wt% of [Mor_{1,15}]Br by employing conductometry, refractive index and surface-tension measurements. The obtained data leads to the determination of the critical micelle concentration values, which have been further used to find various thermodynamic and surface-active parameters of micellization for the investigated system. The modulations observed in the aggregation behavior and the values of obtained parameters are indicative of various interactions prevailing among different constituents of the solution. The knowledge of these interactions is important for the utilization of such systems in various industrial applications such as foams, froths, emulsions, suspensions, and surface coatings to enhance their quality and performance.

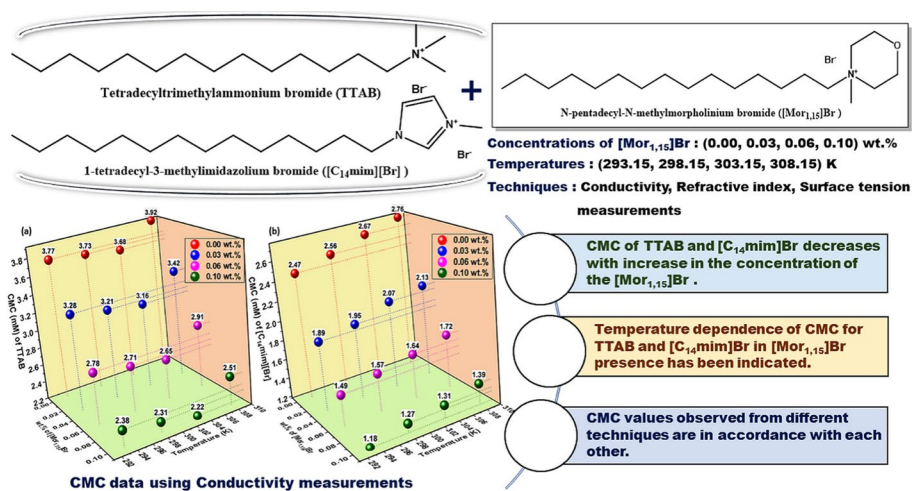
Harsh Kumar—Deceased

✉ Pooja Sharma
poojachem017@gmail.com

Gagandeep Kaur
gagsssethi13@gmail.com

¹ Department of Chemistry, Dr B R Ambedkar National Institute of Technology, Jalandhar, Punjab 144011, India

Graphical Abstract



Keywords TTAB · [C₁₄mim]Br · [Mor_{1,15}][Br] · Micellization · Surface-activity · Micelles · SAILs

1 Introduction

The vast applications of surface-active ionic liquids (SAILs) in different sectors, such as nanomaterials synthesis and separation processing, organic synthesis, micellar catalysis, enhanced oil recovery, water treatment technologies, etc., have piqued researchers' interest [1–6]. Ionic liquids (ILs) have several beneficial and intriguing properties, such as low volatility, exceptional thermal stability, high electric conductivity and wide liquid range [7–10]. The existence of a long hydrophobic chain in ILs makes them surface-active, hence termed SAILs [11–13]. Because SAILs generally contain long hydrophobic alkyl chains, they can self-aggregate into micelles. Micellar aggregation characteristics of SAILs and surfactants have recently gotten a lot of interest from academia and practice [14–17]. Due to the higher stability of SAILs, at high temperatures, than conventional surfactants, the long-chain ILs are able to widen their application regions by mixing the surfactants and ILs. As a result, the self-assembly and aggregation behavior of surfactants or SAILs aided by the ILs addition has a broader use in a variety of domains, including extraction, absorption, separation, and many other practical applications [18–21].

The aggregation of surface-active molecules takes place over a narrow range of concentrations, recognized as the critical micelle concentration (CMC), below which these amphiphilic molecules are primarily distributed as monomers. The value of CMC is very much important in examining the aggregation behavior of surfactants and SAILs, as it provides a great deal of information concerning surface activities and their technological implications. The surface activity of surfactants and SAILs may be altered by the addition of ILs in the solution, which will result in the formation of micelles with interesting features [22–24]. From a practical standpoint, research into such micellar systems incorporating different surfactants and SAILs would overcome various limitations of traditionally used surfactant

systems. This will lead us to broaden the scope of our IL research to include relevant micelle features.

Also, an organic cation and a suitable inorganic or organic anion were usually found in SAILs. Their physicochemical properties may usually be altered for specific applications by introducing appropriate cations and anions into their structure. The diverse organic cation rings, such as alkylmethylimidazolium ($[C_n\text{mim}]^+$), alkylpyridinium ($[C_n\text{Py}]^+$), alkylmethylpiperidinium ($[C_n\text{mpip}]^+$), alkylmethylpyrrolidinium ($[C_n\text{mPyrr}]^+$) and morpholinium ($[C_n\text{Morph}]^+$) can be present in SAILs as reported in the literature, which incorporates unique properties depending upon their cation [25–27]. Our research team has studied the aggregation behavior of several surfactants and SAILs with various additives such as drugs, carbohydrates, vitamins, salts, amino acids, alkylmethylimidazolium-based ILs, etc. [28–31] This, established that the nature of additives and the type of their interactions with the concerned surfactant and SAILs play a significant role in their aggregation. There is no existing report available in the literature that investigates the aggregation behavior of surfactants and SAILs with morpholinium-based SAILs as additives.

Variations in the aggregation behavior of TTAB and $[C_{14}\text{mim}]\text{Br}$ with (0.00, 0.03, 0.06, and 0.10) wt% $[\text{Mor}_{1,15}]\text{Br}$ at temperatures i.e., 293.15–308.15 K with temperature intervals of 5 K, have been observed. The evaluation of CMC, thermodynamic and surface-active parameters revealed the nature of interactions occurring in the micellar systems. The morpholinium-based SAILs i.e., $[\text{Mor}_{1,15}]\text{Br}$ can drastically modify the aggregation of TTAB and $[C_{14}\text{mim}]\text{Br}$, resulting in their improved performance and application in diverse areas.

2 Experimental

2.1 Materials

Chemical names with CAS numbers, structures, sources, and purities of all the compounds used in the study have been enlisted in Table 1.

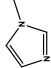
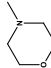
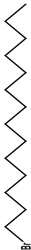




2.1.1 Synthesis of $[C_{14}\text{mim}][\text{Br}]$

For the synthesis of $[C_{14}\text{mim}][\text{Br}]$, the drop-by-drop addition of 1-bromotetradecane to 1-methylimidazole taken in an RB flask was carried out. To facilitate the reaction, acetonitrile was added as a solvent. The reaction mixture was then kept on constant stirring with heating and refluxing at 80 °C for around 48 h. Thin-layer chromatography (TLC) was used to track the reaction's progression to completion. The excess acetonitrile and volatile impurities were removed by using a rotary evaporator. To remove unreacted reactants, the obtained reaction mixture was rinsed with hexane. The obtained product was kept in vacuum desiccators for a few days before use [32–34]. The $^1\text{H-NMR}$ technique has been utilized for its characterization. Figure S1 (SI) shows the obtained $^1\text{H-NMR}$ spectra of synthesized $[C_{14}\text{mim}][\text{Br}]$.

2.1.2 Synthesis of $[\text{Mor}_{1,15}]\text{Br}$

For the synthesis of $[\text{Mor}_{1,15}][\text{Br}]$, 1-bromopentadecane and *N*-methylmorpholine in a 1:1.2 ratio have been taken in the round bottom flask. The toluene was added to the reaction

Table 1 Specification of chemicals

Chemicals	Source	CAS No.	Structure	Purification method	Mass fraction purity
1-Methylimidazole	HiMedia Laboratories Pvt. Ltd., Mumbai, India	616-47-7		No further purification	> 0.99
N-methylmorpholine	Sigma Aldrich	109-02-4		No further purification	0.99
1-Bromotetradecane	TCI Co. Ltd., Tokyo, Japan	112-71-0		No further purification	> 0.97
1-Bromopentadecane	TCI Co. Ltd., Tokyo, Japan	629-72-1		No further purification	> 0.98
Tetradecyltrimethylammonium bromide (TTAB)	Spectrochem Pvt. Ltd., Mumbai, India	1643-19-2		Vacuum drying	> 0.99
Acetonitrile	LOBA Chemie Pvt. Ltd Mumbai, India	75-05-8		No further purification	> 0.995
Hexane	TCI Co. Ltd., Tokyo, Japan	110-54-3		No further purification	> 0.96

#As declared by supplier

mixture as solvent. Then the reaction mixture was kept on continuous stirring and refluxing at approximately 80–90 °C for 48 h under a nitrogen atmosphere. The reaction progress has been monitored by TLC. After the reaction completion, the rotary evaporator was used to evaporate the excess solvent present in the reaction mixture. The resulting product was washed with ethyl acetate. Then the product was placed in desiccators for a few days before use [35, 36]. ¹H-NMR spectra obtained for the [Mor_{1,15}][Br], are shown in Fig. S2 (SI). The synthetic pathways for the [C₁₄mim][Br] and [Mor_{1,15}][Br] synthesis have been indicated in Fig. 1.

2.2 Sample Preparation

The stock solutions of TTAB, [C₁₄mim][Br], and [Mor_{1,15}][Br] have been prepared in the double-distilled water. Double distilled water with the conductivity value $\leq 5 \mu\text{S}\cdot\text{cm}^{-1}$ was obtained using a specialized water purification system i.e., Millipore Milli-Q Academic water purification system. The stock solutions with concentrations (0.00, 0.03, 0.06, and 0.10) wt% of [Mor_{1,15}][Br] have been prepared. These concentrations of [Mor_{1,15}][Br] molecules were chosen so that there may not be the self-assembly of [Mor_{1,15}][Br] molecules in the solution. The accurate weighing of compounds has been carried out using Sartorius CPA 225 D electronic balance (precision ± 0.00001 g). The analysis of obtained data has been conducted using Origin 2018 and MS Excel.

2.3 Methods used

2.3.1 Conductivity Measurements

The specific conductivity of several samples has been measured with a digital conductivity meter (Systronics 306) by using a platinum electrode dipping cell (cell constant = 1.0 cm⁻¹). Aqueous potassium chloride (KCl) solutions in the concentration range (0.01–1.0 mol·kg⁻¹) were used for the instrument's calibration. By multiplying the cell constant by the measured conductivity values, the specific conductivity (κ) values were obtained. Since the cell constant = 1.0 cm⁻¹, the calculated and measured values of specific conductivity (κ) coincide perfectly. The refrigerated circulated water thermostat (accuracy ± 0.1 °C) from Macro Scientific Works Pvt. Ltd. Delhi has been used to sustain the solution temperature. To do this, double walled jacketed cells containing sample solutions are used through which water kept at a certain temperature was circulated. This allows measuring the electrical conductivity of solutions at that particular temperature. To ensure accuracy, all the measurements were carried out in triplicate.

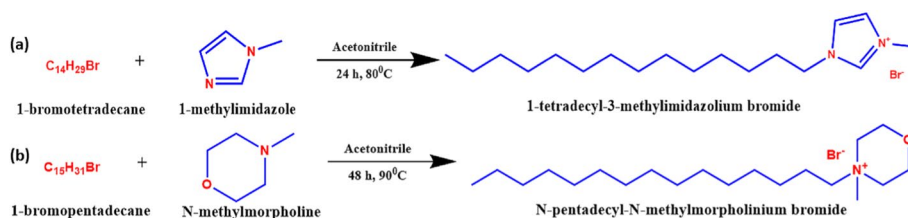


Fig. 1 Synthetic route for the synthesis of **a** [C₁₄mim][Br] and **b** [Mor_{1,15}][Br]

2.3.2 Refractive Index Measurements

Anton Paar's Abbemat 300 refractometer (resolution 0.00001 n_D) is used to measure the refractive index values. Before performing actual measurements, the equipment is calibrated by measuring the refractive index value of water which is 1.3325 n_D at 298.15 K. Internally maintaining the temperature with a temperature probe precision of ± 0.05 °C, the measurements were made at four distinct temperatures (293.15, 298.15, 303.15, 308.15) K. Each measurement is repeated at least three times, with the mean result treated as the final reading (accuracy ± 0.0001 n_D).

2.3.3 Surface Tension Measurements

DCAT 15 tensiometer from DataPhysics Instruments, Germany, was used to measure the values of surface tension at 298.15 K. The DCAT 33 software, combined with the LDU 25 dosing equipment and Wilhelmy plate PT 11, is specifically intended for automatic CMC determination. The temperature is sustained at 298.15 K using a liquid temperature control device TV 70 and a refrigerated circulating water thermostat. The cleaning of plate PT 11 was done by red-burning it with butane gas. Before taking actual measurements, the instrument is calibrated with water, which has a surface tension of 71.99 $\text{mN}\cdot\text{m}^{-1}$ at 298.15 K. Each measurement is made in triplicate, with the average value being used (accuracy ± 0.01 $\text{mN}\cdot\text{m}^{-1}$).

3 Results and Discussion

3.1 Conductivity Measurements

The conductivity data obtained has been utilized to obtain the CMC values and thermodynamic parameters for the aggregation of TTAB and $[\text{C}_{14}\text{mim}]\text{Br}$ with (0.00, 0.03, 0.06, and 0.10) wt% $[\text{Mor}_{1,15}]\text{Br}$ at various temperatures. The data has been analyzed to understand the influence of $[\text{Mor}_{1,15}]\text{Br}$ at various concentrations and temperatures on the aggregation of TTAB and $[\text{C}_{14}\text{mim}]\text{Br}$.

3.1.1 Critical Micelle Concentration (CMC)

The obtained specific conductivity values for the aqueous solutions of TTAB and $[\text{C}_{14}\text{mim}]\text{Br}$ with (0.00, 0.03, 0.06, and 0.10) wt% $[\text{Mor}_{1,15}]\text{Br}$ at various temperatures are utilized to determine the CMC values. The obtained values of specific conductivity for various solutions at (293.15, 298.15, 303.15, and 308.15) K have been reported in Table S1–3 shown in supporting information. The CMC values have been obtained by plotting the specific conductivity versus the concentration for various solutions, which have been shown in Figs. 2 and 3. It can be detected from the obtained plots, that specific conductivity values increase with the concentration of TTAB and $[\text{C}_{14}\text{mim}]\text{Br}$ in the solution. When the concentration approaches the specific concentration i.e., CMC, the micelle formation takes place. Then, the rate of change in conductivity decreases with the increasing concentration of TTAB and $[\text{C}_{14}\text{mim}]\text{Br}$ with (0.00, 0.03, 0.06, and 0.10) wt% $[\text{Mor}_{1,15}]\text{Br}$, resulting in a lower

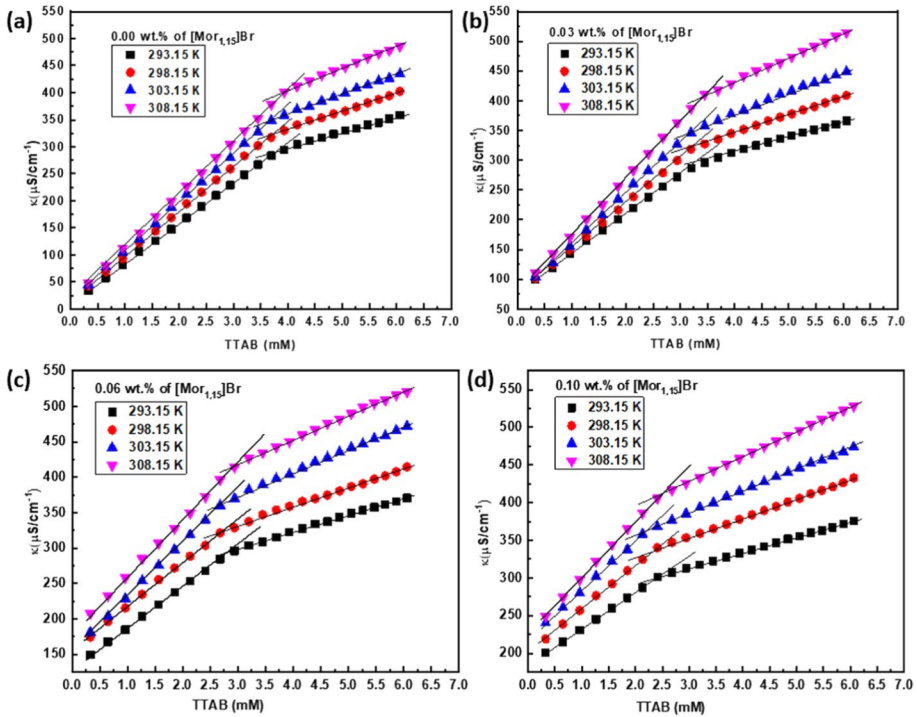


Fig. 2 Plot of specific conductance versus varying concentrations of TTAB in **a** 0.00 wt% **b** 0.03 wt% **c** 0.06 wt% and **d** 0.10 wt% of $[\text{Mor}_{1,15}]\text{Br}$ at different temperatures in aqueous media

slope for the line in the post-micellar region than in the pre-micellar region. The slope of the pre-micellar region (S_1) and the post-micellar region (S_2) have been employed to determine the degree of counterion dissociation (α) by using Eq. 1.

$$\alpha = S_2/S_1 \quad (1)$$

The variation in the slopes is due to the fact that the charge carriers become fewer on micelle formation [22, 37]. The loss of charge carriers after micelle formation is because the counterions get attached to the micellar surface. Also, the formed micelles exhibit lower mobility as compared to free surfactant monomers, further slowing the charge transport. Thus, a breakpoint is observed in conductivity versus concentration plots [38, 39].

The concentrations of surface-active molecules corresponding to the breakpoint at different temperatures give the values of CMC for TTAB and $[\text{C}_{14}\text{mim}]\text{Br}$ with (0.00, 0.03, 0.06, and 0.10) wt% $[\text{Mor}_{1,15}]\text{Br}$, as indicated in Table 2. The addition of $[\text{Mor}_{1,15}]\text{Br}$ at various concentrations and temperatures has been shown to significantly modulate the micellization behavior of TTAB and $[\text{C}_{14}\text{mim}]\text{Br}$ in aqueous media.

3.1.1.1 Effect of Adding $[\text{Mor}_{1,15}]\text{Br}$ at Different Concentrations The micelle formation tendency of TTAB and $[\text{C}_{14}\text{mim}]\text{Br}$ enhances with the concentration of $[\text{Mor}_{1,15}]\text{Br}$ in solution at all investigated temperatures. This is due to the existence of favorable interactions among the monomers of TTAB and $[\text{C}_{14}\text{mim}]\text{Br}$ when $[\text{Mor}_{1,15}]\text{Br}$ is added to the solution. The strong hydrophobic interactions occur between the hydrophobic chains of TTAB, which

Table 2 Thermodynamic parameters of micellization for TTAB and [C₁₄mim][Br] in (0.00, 0.03, 0.06 and 0.10) wt% of [Mor_{1,15}Br] at different temperatures in aqueous media

[Mor _{1,15} Br]/wt%	Temperature/K	CMC (mmol·L ⁻¹)	α	ΔG_m^0 (kJ·mol ⁻¹)	ΔH_m^0 (kJ·mol ⁻¹)	ΔS_m^0 (kJ·mol ⁻¹)
TTAB						
0.00	293.15	3.77	0.385	-37.79	-2.39	120.76
	298.15	3.73	0.392	-38.31	-2.46	120.24
	303.15	3.68	0.398	-38.85	-2.53	119.79
	308.15	3.92	0.404	-39.09	-2.61	118.37
0.03	293.15	3.28	0.395	-38.09	-2.52	121.36
	298.15	3.21	0.403	-38.63	-2.59	120.88
	303.15	3.16	0.409	-39.20	-2.67	120.51
	308.15	3.42	0.414	-39.40	-2.75	118.94
0.06	293.15	2.78	0.409	-38.41	-2.61	122.14
	298.15	2.71	0.417	-38.96	-2.68	121.66
	303.15	2.64	0.423	-39.55	-2.76	121.34
	308.15	2.91	0.427	-39.73	-2.85	119.68
0.10	293.15	2.38	0.421	-38.71	-2.70	122.83
	298.15	2.31	0.428	-39.33	-2.78	122.57
	303.15	2.22	0.436	-39.93	-2.86	122.26
	308.15	2.51	0.441	-39.96	-2.95	120.10
[C ₁₄ mim][Br]						
0.00	293.15	2.47	0.281	-41.98	-9.21	111.77
	298.15	2.56	0.301	-42.06	-9.42	109.47
	303.15	2.67	0.320	-42.10	-9.63	107.12
	308.15	2.76	0.339	-42.17	-9.84	104.93
0.03	293.15	1.89	0.289	-42.91	-10.23	111.49
	298.15	1.95	0.309	-43.01	-10.46	109.18
	303.15	2.07	0.325	-43.05	-10.71	106.72
	308.15	2.13	0.345	-43.11	-10.93	104.46
0.06	293.15	1.49	0.299	-43.63	-11.53	109.55
	298.15	1.57	0.314	-43.77	-11.82	107.19
	303.15	1.64	0.331	-43.87	-12.09	104.84
	308.15	1.72	0.349	-43.93	-12.37	102.45
0.10	293.15	1.18	0.306	-44.44	-12.65	108.45
	298.15	1.27	0.319	-44.53	-12.98	105.85
	303.15	1.31	0.337	-44.66	-13.28	103.56
	308.15	1.39	0.352	-44.73	-13.59	101.07

Standard uncertainties s are $s(T) = \pm 0.1$ K, $s(\text{CMC}) = \pm 0.01$ mmol·L⁻¹, $s(\Delta G_m^0) = \pm 0.03$ kJ·mol⁻¹, $s(\Delta H_m^0) = \pm 0.02$ kJ·mol⁻¹, $s(\Delta S_m^0) = \pm 0.02$ J·mol⁻¹·K⁻¹

lead to the formation of micellar aggregates in the solution. The existence of strong electrostatic attraction among the trimethylammonium ($-N^+(\text{CH}_3)_3$) head groups of TTAB and Br⁻ counterions facilitates micelle formation by masking the electrostatic repulsive interactions among the similarly charged cationic head groups of TTAB [40]. The addition of [Mor_{1,15}] Br in the solution of TTAB facilitates micelle formation as the long alkyl chains of [Mor_{1,15}]

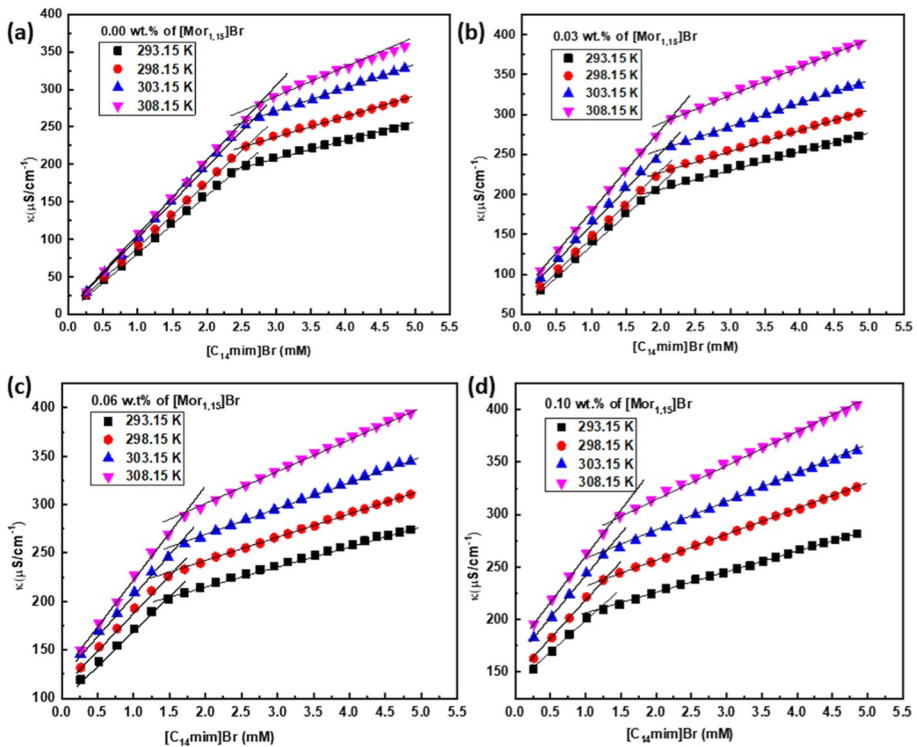


Fig. 3 Plot of specific conductance versus varying concentrations of $[C_{14}mim]Br$ in **a** 0.00 wt% **b** 0.03 wt% **c** 0.06 wt% and **d** 0.10 wt% of $[Mor_{1,15}]Br$ at different temperatures in aqueous media

Br starts interacting with the alkyl chains of TTAB, thereby reducing the CMC values of TTAB with the increase in concentrations of $[Mor_{1,15}]Br$ in solution at all temperatures [41]. Similarly, the CMC values of $[C_{14}mim]Br$ in aqueous media also decrease with the addition of $[Mor_{1,15}]Br$ in the solution. The existence of electrostatic repulsive interactions among similarly charged imidazolium cation-based head groups of $[C_{14}mim]Br$ gets compensated with the existence of counterions. The hydrophobic interactions occurring among the alkyl chains of $[C_{14}mim]Br$ and $[Mor_{1,15}]Br$ and hydrogen bonding interactions prevailing between the head groups of $[C_{14}mim]Br$ and $[Mor_{1,15}]Br$ over the micellar surface contribute to enhancing the micellization tendency of $[C_{14}mim]Br$ with $[Mor_{1,15}]Br$ as an additive at various concentrations in solution [42]. The increase in concentrations of $[Mor_{1,15}]Br$ leads to enhance the micellization tendency of TTAB and $[C_{14}mim]Br$ in aqueous media as evident from the obtained CMC values at all investigated temperatures.

3.1.1.2 Effect of Varying Temperature on Micellization The temperature has been shown to influence the micellization tendency of TTAB and $[C_{14}mim]Br$ in a significant way. As observed in Table 2, the CMC values of TTAB decrease with an increase in temperature as the temperature is raised from 293.15 to 303.15 K. After 303.15 K, the CMC value for TTAB starts increasing as the temperature is increased to 308.15 K. Similar trend in the CMC variation of TTAB in (0.00, 0.03, 0.06 and 0.10) wt% of $[Mor_{1,15}]Br$ in solution with the temperature change has been observed. Thus, the CMC values of TTAB represent a

U-type behavior in the range of 293.15 to 308.15 K. On the other side, the values of CMC for $[C_{14}mim]Br$ increases with temperature increase in the range of 293.15 to 308.15 K as observed in the presence of (0.00, 0.03, 0.06, and 0.10) wt% of $[Mor_{1,15}]Br$ in solution. The observed behavior in the micelle forming tendency of investigated systems with the temperature variation can be explained based on two opposing effects. (i) As the temperature rises, there may be a decrease in the hydration of hydrophilic head groups present in surface-active monomers. This results in the enhancement of micellization tendency, which results in the CMC value decrease. (ii) However, as the temperature rises, the structured water surrounding the hydrophobic group is also disrupted, making micellization more difficult. This is due to the solubilization of surface-active molecules in water and the value of CMC increases. Thus, in the case of a particular surface-active agent, the CMC variation with temperature depends upon the dominance of any one of the effects over the other [43, 44]. In the case of TTAB, the first effect dominates in the range 293.15–303.15 K, whereas the second effect dominates above 303.15 K. Thus, the CMC values of TTAB with $[Mor_{1,15}]Br$ in solution initially decrease from 293.15 to 303.15 K, and then start increasing as the temperature rises above 303.15 K as indicated in Fig. 4a. In the case of $[C_{14}mim]Br$ with $[Mor_{1,15}]Br$ in solution, the second effect dominates in the entire investigated temperature range i.e., from 293.15 to 308.15 K, leading to retard the micelle formation of $[C_{14}mim]Br$ with temperature elevation in (0.00, 0.03, 0.06 and 0.10) wt% $[Mor_{1,15}]Br$ in solution. Thus, the CMC values of $[C_{14}mim]Br$ with $[Mor_{1,15}]Br$ in solution increase with the increase in temperature as indicated in Fig. 4b.

3.1.2 Thermodynamic Parameters of Micellization: Standard Free Energy of Micellization (ΔG_m^0), Standard Enthalpy of Micellization (ΔH_m^0), Standard Entropy of Micellization (ΔS_m^0)

The obtained values of CMC and α have been further employed to calculate different thermodynamic parameters of micellization i.e., standard free energy of micellization (ΔG_m^0), standard enthalpy of micellization (ΔH_m^0), and standard entropy of micellization (ΔS_m^0) [45, 46].

The standard free energy of micellization (ΔG_m^0) can be calculated as

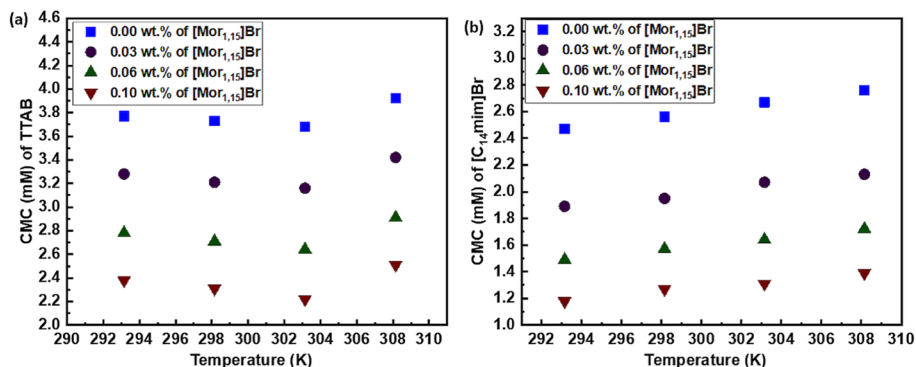


Fig. 4 Variation in CMC values of **a** TTAB **b** $[C_{14}mim][Br]$ with temperature in (0.00, 0.03, 0.06 and 0.10) wt% of $[Mor_{1,15}]Br$ in aqueous media

$$\Delta G_m^0 = (2 - \alpha)RT(\ln X_{\text{CMC}}) \quad (2)$$

The standard enthalpy of micellization (ΔH_m^0) can be calculated as

$$\Delta H_m^0 = -RT^2(2 - \alpha) \left[\frac{d(\ln X_{\text{CMC}})}{dT} \right] \quad (3)$$

The standard entropy of micellization (ΔS_m^0) can be calculated as

$$\Delta S_m^0 = (\Delta H_m^0 - \Delta G_m^0)/T \quad (4)$$

where R is the universal gas constant, T represents temperature, X_{CMC} denotes the CMC in the mole fraction units. The determined values for ΔG_m^0 , ΔH_m^0 and ΔS_m^0 at different temperature for the micellization of TTAB and [C₁₄mim]Br in (0.00, 0.03, 0.06, and 0.10) wt% [Mor_{1,15}] are reported in Table 2. Figures S3–5 given in supporting information indicate the change in the values of these parameters with the variation in temperature and concentrations of [Mor_{1,15}]Br in solution. The negative ΔG_m^0 values obtained for the micellization of TTAB and [C₁₄mim]Br at all investigated temperatures and concentrations of [Mor_{1,15}]Br indicate the spontaneous micelle formation. The more negative values of ΔG_m^0 at higher concentrations of [Mor_{1,15}]Br have been obtained indicating greater spontaneity and feasibility in the micellization of TTAB and [C₁₄mim]Br with the addition of [Mor_{1,15}]Br in solution. The monomers of [Mor_{1,15}]Br interacts with the monomers of TTAB and [C₁₄mim]Br in such a way that leads to enhance their micellization tendency. An analogous trend has been obtained for the ΔH_m^0 values, where the obtained negative values ΔH_m^0 specify the exothermic nature for the micellization of TTAB and [C₁₄mim]Br with and without [Mor_{1,15}]Br in solution. The ΔS_m^0 values have been obtained positive in all the cases, whose values decrease with the rise in temperature for both TTAB and [C₁₄mim]Br at various [Mor_{1,15}]Br concentrations. The values of ΔS_m^0 have been observed to increase for TTAB, whereas these values decrease for [C₁₄mim]Br with the increase in [Mor_{1,15}]Br concentration. The obtained negative values of ΔH_m^0 and positive values of ΔS_m^0 contribute to the negative values obtained for ΔG_m^0 in case of TTAB and [C₁₄mim]Br in the absence and presence of [Mor_{1,15}]Br in solution. The higher contribution of ΔS_m^0 as compared to ΔH_m^0 towards the obtained negative values of ΔG_m^0 has been observed in all the cases. This is because $-T\Delta S_m^0$ has been obtained higher as compared to ΔH_m^0 , which signifies the entropy-driven process of micellization. It means that the structured water clusters around the hydrophobic tails of TTAB and [C₁₄mim]Br monomers in solution get distorted upon micelle formation, due to the “hiding” of non-polar hydrocarbon alkyl chains inside the micellar core. This leads to the release of water molecules which results in more positive ΔS_m^0 values for the micellization of TTAB and [C₁₄mim]Br with and without [Mor_{1,15}]Br in solution.

3.2 Refractive Index Measurements

The refractive index is the quantity that measures how a light beam bends as it goes through one medium to the other. The measurement of refractive index at different concentrations of surface-active molecules can also be used to calculate their CMC values. This is owing to the fact that the refractive index of monomers is lower than that of produced micelles. Thus, the refractive index values for TTAB and [C₁₄mim]Br in (0.00, 0.03, 0.06, and 0.10)

wt% $[\text{Mor}_{1,15}]\text{Br}$ have been measured at different temperatures as reported in Tables S4–6 given in supporting information.

To obtain the CMC values, the refractive index values have been used, which were plotted against the concentration of TTAB and $[\text{C}_{14}\text{mim}]\text{Br}$ in (0.00, 0.03, 0.06, and 0.10) wt% $[\text{Mor}_{1,15}]\text{Br}$ as indicated in Figs. 5 and 6, respectively.

Figures show that the refractive index values increase rapidly with the concentration of TTAB and $[\text{C}_{14}\text{mim}]\text{Br}$ in (0.00, 0.03, 0.06, and 0.10) wt% $[\text{Mor}_{1,15}]\text{Br}$, when the concentration is below CMC value. But as the concentration approaches CMC, the rate of increase of refractive index with the increase in concentration decreases [47–49]. As a result, the breakpoint appears in the refractive index versus concentration plots of TTAB and $[\text{C}_{14}\text{mim}]\text{Br}$ with and without $[\text{Mor}_{1,15}]\text{Br}$. The values of CMC for the investigated systems have been obtained at concentration consistent with the breakpoint. Table 3 displays the comparison between the CMC values acquired using this method and those obtained by conductivity measurements. The measurements of CMC values using the refractive index measurement technique correlate well with conductivity-based estimates.

3.3 Surface Tension Measurements

The surface tension measurement technique is another convenient approach that aids in examining the aggregation behavior of surface-active molecules and also provides crucial details regarding the adsorption process occurring at the interface. Thus, the self-assembly, aggregation and interfacial behavior along with the probable interactions which occur

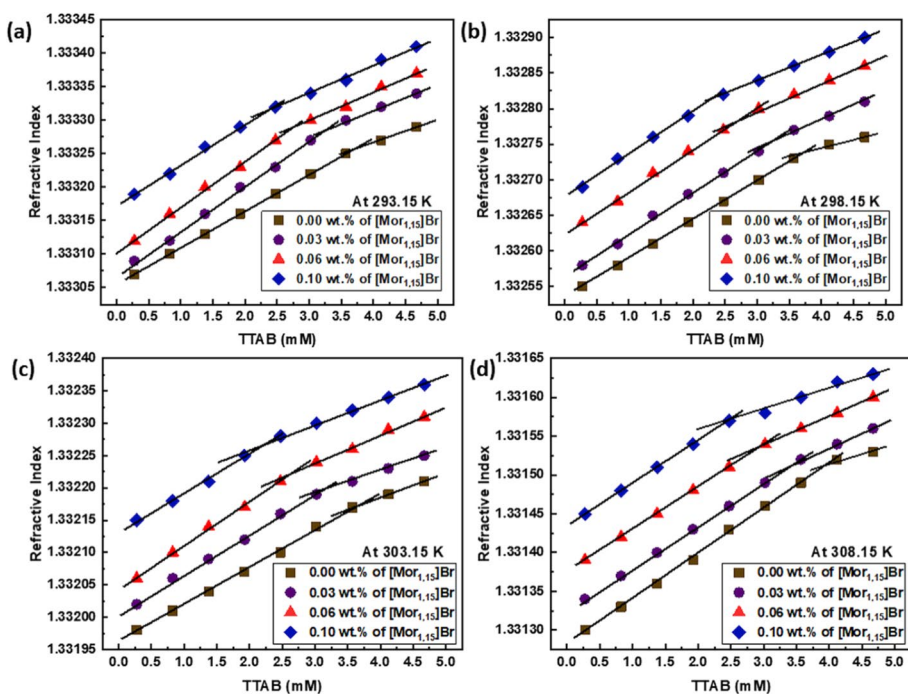


Fig. 5 Plots of refractive index versus varying concentrations of TTAB in (0.00, 0.03, 0.06 and 0.10) wt% of $[\text{Mor}_{1,15}]\text{Br}$ at **a** 293.15 K **b** 298.15 K **c** 303.15 K and **d** 308.15 K in aqueous media

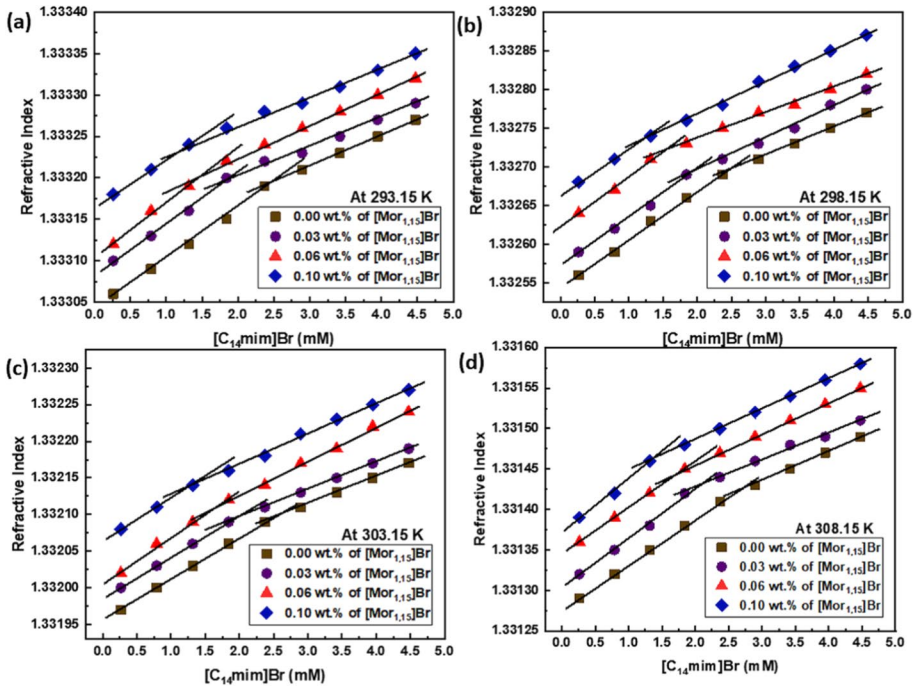


Fig. 6 Plots of refractive index versus varying concentrations of $[C_{14}mim]Br$ in (0.00, 0.03, 0.06 and 0.10) wt% of $[Mor_{1,15}]Br$ at **a** 293.15 K **b** 298.15 K **c** 303.15 K and **d** 308.15 K in aqueous media

Table 3 Comparison of CMC values obtained for TTAB and $[C_{14}mim]Br$ in (0.00, 0.03, 0.06 and 0.10) wt% of $[Mor_{1,15}]Br$ at different temperatures using different techniques

[Mor _{1,15}]Br/wt%	Temperature /K	CMC (mmol·L ⁻¹) for TTAB		CMC (mmol·L ⁻¹) for [C ₁₄ mim] [Br]	
		Conductivity	Refractive index	Conductivity	Refractive index
0.00	293.15	3.77	3.75	2.47	2.45
	298.15	3.73	3.72	2.56	2.52
	303.15	3.68	3.65	2.67	2.63
	308.15	3.92	3.91	2.76	2.74
0.03	293.15	3.28	3.26	1.89	1.86
	298.15	3.21	3.20	1.95	1.93
	303.15	3.16	3.15	2.07	2.04
	308.15	3.42	3.41	2.13	2.12
0.06	293.15	2.78	2.77	1.49	1.46
	298.15	2.71	2.69	1.57	1.55
	303.15	2.64	2.63	1.64	1.63
	308.15	2.91	2.90	1.72	1.71
0.10	293.15	2.38	2.36	1.18	1.16
	298.15	2.31	2.29	1.27	1.24
	303.15	2.22	2.20	1.31	1.29
	308.15	2.51	2.49	1.39	1.37

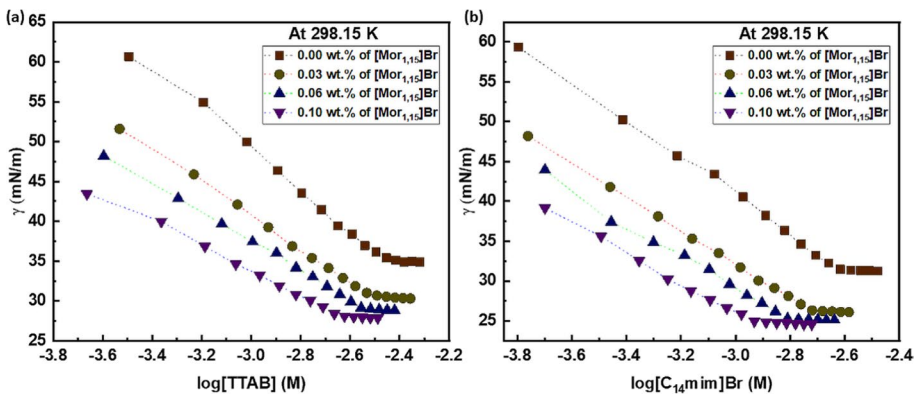
Standard uncertainties s are $s(T) = \pm 0.1$ K, $s(CMC) = \pm 0.01$ mmol·L⁻¹

Table 4 Surface active parameters of TTAB and [C₁₄mim][Br] in (0.00, 0.03, 0.06 and 0.10) wt% of [Mor_{1,15}]Br in aqueous solution at 298.15 K

[Mor _{1,15}]Br (wt%)	CMC (mmol·L ⁻¹) by surface tension	γ_{CMC} (mN·m ⁻¹)	Π_{CMC}	10^6 (mol·m ⁻²)	A_{min} (nm ²)	ΔG_{ad}^0 (kJ·mol ⁻¹)	G_{min}^s (kJ·mol ⁻¹)	Packing parameter (p)
TTAB								
0.00	3.70	35.28	36.71	2.41	0.69	-53.52	14.61	0.31
0.03	3.20	30.72	35.01	1.89	0.88	-57.18	16.28	0.24
0.06	2.70	29.24	32.01	1.71	0.97	-57.64	17.06	0.22
0.10	2.28	28.28	28.46	1.52	1.09	-58.06	18.61	0.19
[C ₁₄ mim][Br]								
0.00	2.53	31.41	40.58	2.28	0.73	-59.89	13.80	0.29
0.03	1.93	26.28	39.45	1.81	0.92	-64.79	14.51	0.23
0.06	1.56	25.27	35.98	1.62	1.02	-65.93	15.56	0.21
0.10	1.25	24.88	31.86	1.45	1.14	-66.48	17.13	0.18

Standard uncertainties s are $s(T) = \pm 0.1$ °C, $s(\text{CMC}) = \pm 0.01$ mmol·L⁻¹, $s(\gamma_{\text{cmc}}) = \pm 0.1$ mN·m⁻¹, $s(\Pi_{\text{cmc}}) = \pm 0.1$ mN·m⁻¹, $s(\Gamma_{\text{max}}) = \pm 0.01$ μmol·m⁻², $s(A_{\text{min}}) = \pm 0.02$ nm², $s(\Delta G_{\text{ad}}^0) = \pm 0.02$ kJ·mol⁻¹, $s(G_{\text{min}}^s) = \pm 0.02$ kJ·mol⁻¹

among various components of the solution have been investigated using the surface tension method [14, 50]. The surface tension (γ) values of the aqueous TTAB and [C₁₄mim]Br in the [Mor_{1,15}]Br solutions were measured to determine their surface activity and CMC values. The surface tension (γ) values for TTAB and [C₁₄mim]Br in (0.00, 0.03, 0.06, and 0.10) wt% [Mor_{1,15}]Br have been reported in Tables S7 and S8, respectively, given in supporting information. Figure 7 represents the surface tension versus the logarithm of TTAB and [C₁₄mim]Br concentration plots with and without the addition of various concentrations of [Mor_{1,15}]Br in solution. It is evident from the figure that, at higher concentrations of surface-active molecules, the surface tension gradually decreases as the concentration rises; this suggests that surface-active molecules are adsorbed at the air/solution interface.

**Fig. 7** Plots of surface tension versus logarithm of concentrations **a** TTAB **b** [C₁₄mim] [Br] in (0.00, 0.03, 0.06 and 0.10) wt% of [Mor_{1,15}]Br at 298.15 K in aqueous media

As the concentration of surface-active molecules approaches the CMC value, the γ values become approximately constant yielding a breakpoint in the plot. Thus, the CMC value is obtained at the concentration coinciding with the breakpoint [51, 52]. The obtained data for surface tension has been further employed to determine various surface-active parameters for the concerned systems as indicated in Table 4.

The surface pressure at CMC (Π_{CMC}) has been calculated as follows.

$$\Pi_{\text{CMC}} = \gamma_0 - \gamma_{\text{CMC}} \quad (5)$$

where γ_0 represents surface tension of solvent in pure state and γ_{CMC} represents the surface tension of solution at CMC. The maximum surface excess concentration (Γ_{max}) and minimum area of surfactant monomer at the air/solution interface (A_{min}) have been evaluated by applying the following equations.

$$\Gamma_{\text{max}} = -\frac{1}{RT} \left(\frac{\partial \gamma}{\partial (\ln C)} \right) \quad (6)$$

$$A_{\text{min}} = \frac{1}{N_A \Gamma_{\text{max}}} \quad (7)$$

where T is the temperature, R is the universal gas constant, C is the concentration of the solution, N_A represents the Avogadro's Number i.e., $6.022 \times 10^{23} \text{ mol}^{-1}$.

The standard Gibbs free energy of adsorption (ΔG_{ad}^0) and the free energy of a surface at equilibrium (G_{min}^s), proposed by Sugihara et al. have been calculated as follows.

$$\Delta G_{\text{ad}}^0 = \Delta G_m^0 - \frac{\Pi_{\text{CMC}}}{\Gamma_{\text{max}}} \quad (8)$$

$$G_{\text{min}}^s = A_{\text{min}} \gamma_{\text{CMC}} N_A \quad (9)$$

where ΔG_m^0 is the standard Gibbs free energy of micellization as determined by using Eq. 2.

The value of the packing parameter (p) has also been evaluated as follows.

$$p = V_0 / l_c A_{\text{min}} \quad (10)$$

where V_0 indicates the volume occupied by the hydrophobic group in the micellar core, l_c represents the length of the hydrophobic core. The values of V_0 and l_c can be determined by using Tanford's formulae.

$$V_0 = [27.4 + 26.9(n_c - 1)] (\text{\AA}^3) \quad (11)$$

$$l_c = [1.54 + 1.26(n_c - 1)] (\text{\AA}) \quad (12)$$

Here, n_c represents the total number of carbons in the hydrocarbon chain of the surface active agent.

The careful analysis of Table 4 indicates the proximity in the CMC values obtained by different techniques. The addition of [Mor_{1,15}]Br at various concentrations in the solutions of TTAB and [C₁₄mim]Br results in a decrease in values of γ_{CMC} , indicating a rise in surface activity of the solution. The greater surface-activity of [C₁₄mim]Br has been detected than TTAB as specified by the obtained lesser values of γ_{CMC} in case of [C₁₄mim]Br as compared to TTAB in (0.00, 0.03, 0.06 and 0.10) wt% [Mor_{1,15}]Br. The values of Γ_{max} and A_{min} provides the knowledge of orientation and packing of surface-active monomers at the air/solution interface [53, 54]. The addition of [Mor_{1,15}]Br at higher concentrations in the solution of TTAB and [C₁₄mim]Br results in the decrease in values of Γ_{max} and the increase in the values of A_{min} . This trend in the values of Γ_{max} and A_{min} indicate loose packing of TTAB and [C₁₄mim]Br monomers at air/solution interface with the rise in [Mor_{1,15}]Br concentration. Also, the lesser value of Γ_{max} for [C₁₄mim]Br as compared to TTAB with and without [Mor_{1,15}]Br indicates loose packing of [C₁₄mim]Br monomers at the interface as compared to that of TTAB. The values of Γ_{max} and A_{min} primarily depend on (a) the attractive or van der Waals interactions that exist between the hydrophobic parts of the [Mor_{1,15}]Br with TTAB and [C₁₄mim]Br in TTAB/[Mor_{1,15}]Br and [C₁₄mim]Br/[Mor_{1,15}]Br system, respectively and (b) the steric hindrance brought on by the bulky groups present in various interacting species. The hydrophobic part of [Mor_{1,15}]Br monomers can be used to explain the observed decrease in Γ_{max} as the concentration of [Mor_{1,15}]Br increases in the solution. The hydrophobic alkyl chains of [Mor_{1,15}]Br avoid making contact with polar water molecules, thus, tend to concentrate in substantial amounts at the interface, and obstruct the adsorption in TTAB/[Mor_{1,15}]Br and [C₁₄mim]Br/[Mor_{1,15}]Br system, respectively. Thus, the loose packing of TTAB and [C₁₄mim]Br in respective TTAB/[Mor_{1,15}]Br and [C₁₄mim]Br/[Mor_{1,15}]Br systems has been observed at the interface as evident from the obtained values of Γ_{max} and A_{min} . The negative values of ΔG_{ad}^0 have been obtained for pure TTAB, pure [C₁₄mim]Br, TTAB/[Mor_{1,15}]Br mixtures and [C₁₄mim]Br/[Mor_{1,15}]Br mixtures. On comparing ΔG_{ad}^0 and ΔG_m^0 , it is observed that the former has a higher negative value than the latter, indicating that the adsorption process is preferable to the micellization process [51]. Thus, adsorption is the primary process, whereas micellization is the secondary process as some work required the transportation of surfactant monomers from their monomeric form at the surface to their micellar form in the aqueous solution. The ΔG_{ad} values have been observed to attain more negative values in the case of TTAB/[Mor_{1,15}]Br mixtures and [C₁₄mim]Br/[Mor_{1,15}]Br mixtures as compared to pure TTAB and pure [C₁₄mim]Br solutions. This indicates the greater spontaneity of monomer adsorption for TTAB and [C₁₄mim]Br monomers in TTAB/[Mor_{1,15}]Br and [C₁₄mim]Br/[Mor_{1,15}]Br mixtures, respectively. The obtained positive values of G_{min}^s in the investigated systems indicates the formation of thermodynamically stable surfaces and micelles in solutions of TTAB/[Mor_{1,15}]Br and [C₁₄mim]Br/[Mor_{1,15}]Br. The values of the packing parameter (p) indicate the formed micelles in the concerned systems to be spherically shaped as the value of p lies between 0 and 0.33 [55].

4 Conclusion

The aggregation behavior of TTAB and [C₁₄mim]Br in (0.00, 0.03, 0.06, and 0.10) wt% [Mor_{1,15}]Br has been analyzed to get insight into the interactions prevailing in TTAB/[Mor_{1,15}]Br and [C₁₄mim]Br/[Mor_{1,15}]Br mixtures. Conductivity, refractive index, and surface tension measurement techniques have been used to evaluate various parameters such

as critical micelle concentration (CMC), the standard free energy of micellization (ΔG_m^0), standard enthalpy of micellization (ΔH_m^0), and standard entropy of micellization (ΔS_m^0), surface pressure at *cmc* (Π_{CMC}), maximum surface excess concentration (Γ_{max}), the minimum area of surfactant monomer at the air/solution interface (A_{min}), standard Gibbs free energy of adsorption (ΔG_{ad}^0), the free energy of a surface at equilibrium (G_{min}^s) and packing parameter (p). The values of CMC and other evaluated parameters for the investigated systems get altered with the temperature and the concentration of [Mor_{1,15}]Br in the solution. The values of all the parameters obtained for TTAB/[Mor_{1,15}]Br and [C₁₄mim]Br/[Mor_{1,15}]Br mixtures have been compared to analyze the aggregation behavior of TTAB and [C₁₄mim]Br with [Mor_{1,15}]Br at various concentrations in aqueous media. The superior surface activity has been observed for [C₁₄mim]Br as compared to TTAB with and without [Mor_{1,15}]Br in solution at various concentrations and temperatures.

Supplementary Information The online version contains supplementary material available at <https://doi.org/10.1007/s10953-023-01299-8>.

Acknowledgements Authors acknowledge the Director and Head, Department of Chemistry Dr. B.R. Ambedkar National Institute of Technology for necessary facilities. One of the authors, Gagandeep Kaur is thankful to Department of Science and Technology (DST) of New Delhi for providing financial support via DST INSPIRE Fellowship (IF170753).

Author Contributions Gagandeep Kaur planned the experiments, analysed the data and wrote the paper. All authors contributed to the manuscript revision, and read and approved the submitted version.

Declarations

Competing interests The authors declare no competing interests.

References

1. Huang, W., Wu, X., Qi, J., Zhu, Q., Wu, W., Lu, Y., Chen, Z.: Ionic liquids: green and tailor-made solvents in drug delivery. *Drug Discov. Today*. **25**, 901–908 (2020). <https://doi.org/10.1016/J.DRUDIS.2019.09.018>
2. Dutta, R., Kundu, S., Sarkar, N.: Ionic liquid-induced aggregate formation and their applications. *Bio-phys. Rev.* **10**, 861–871 (2018). <https://doi.org/10.1007/s12551-018-0408-5>
3. Toledo Hijo, A.A.C., Maximo, G.J., Costa, M.C., Batista, E.A.C., Meirelles, A.J.A.: Applications of ionic liquids in the food and bioproducts industries. *ACS Sustain. Chem. Eng.* **4**, 5347–5369 (2016). <https://doi.org/10.1021/acssuschemeng.6b00560>
4. Wasilewski, T.: Ionic liquids in gas sensors and biosensors. In: *Green Sustainable Process for Chemical and Environmental Engineering and Science: Ionic Liquids as Green Solvents*, pp. 287–318. Elsevier Inc, Amsterdam (2019)
5. Mahura, T., Bahadur, I., Naidoo, P., Ramjugernath, D.: Probing the ion–dipole interactions between the imidazolium-based ionic liquids and polyethylene glycol 200 using excess thermodynamic and spectroscopy studies. *J. Mol. Liq.* **350**, 118519 (2022). <https://doi.org/10.1016/j.molliq.2022.118519>
6. Masilo, K., Singh, S.K., Bahadur, I.: Interactions between 1-butyl-3-methylimidazolium cation with various anions and carboxylic acids: physicochemical and spectroscopic aspects. *Colloids Surf. Physicochem. Eng. Asp.* **617**, 126376 (2021). <https://doi.org/10.1016/j.colsurfa.2021.126376>
7. Brennecke, J.F., Maginn, E.J.: Ionic liquids: innovative fluids for chemical processing. *AIChE J.* **47**, 2384–2389 (2001). <https://doi.org/10.1002/aic.690471102>
8. Chiappe, C., Pieraccini, D.: Ionic liquids: solvent properties and organic reactivity. *J. Phys. Org. Chem.* **18**, 275–297 (2005). <https://doi.org/10.1002/poc.863>
9. Giernoth, R.: Task-specific ionic liquids. *Angew. Chem. Int. Ed.* **49**, 2834–2839 (2010). <https://doi.org/10.1002/anie.200905981>

10. Rogers, R.D., Seddon, K.R.: Ionic liquids—solvents of the future? *Science* **80**(302), 792–793 (2003). <https://doi.org/10.1126/science.1090313>
11. Garcia, M.T., Ribosa, I., González, J.J., Comelles, F.: Surface activity, self-aggregation and antimicrobial activity of catanionic mixtures of surface active imidazolium- or pyridinium-based ionic liquids and sodium bis(2-ethylhexyl) sulfosuccinate. *J. Mol. Liq.* **303**, 112637 (2020). <https://doi.org/10.1016/j.molliq.2020.112637>
12. Kumar, H., Kaur, G.: Scrutinizing self-assembly, surface activity and aggregation behavior of mixtures of imidazolium based ionic liquids and surfactants: a comprehensive review. *Front. Chem.* (2021). <https://doi.org/10.3389/fchem.2021.667941>
13. El Seoud, O.A., Keppeler, N., Malek, N.I., Galgano, P.D.: Ionic liquid-based surfactants: recent advances in their syntheses, solution properties, and applications. *Polymers (Basel)* **13**, 1100 (2021). <https://doi.org/10.3390/polym13071100>
14. Pal, A., Saini, M.: Thermodynamic and micellization behavior of long chain 1-octyl-2,3-dimethylimidazolium bromide [omim][Br] in aqueous solution in the absence and in presence of a series of alkali salts. *J. Dispers. Sci. Technol.* **40**, 1197–1204 (2019). <https://doi.org/10.1080/01932691.2018.1503546>
15. Srinivasa Rao, K., Gehlot, P.S., Trivedi, T.J., Kumar, A.: Self-assembly of new surface active ionic liquids based on Aerosol-OT in aqueous media. *J. Colloid Interface Sci.* **428**, 267–275 (2014). <https://doi.org/10.1016/j.jcis.2014.04.062>
16. Dong, B., Li, N., Zheng, L., Yu, L.: Surface adsorption and micelle formation of surface active ionic liquids in aqueous solution. *Langmuir*. **23**, 4178–4182 (2007). <https://doi.org/10.1016/j.jcis.2012.09.073>
17. Chauhan, S., Kaur, M., Singh, K., Chauhan, M.S., Kohli, P.: Micellar and antimicrobial activities of ionic surfactants in aqueous solutions of synthesized tetraalkylammonium based ionic liquids. *Colloids Surf. Physicochem. Eng. Asp.* **535**, 232–241 (2017). <https://doi.org/10.1016/j.colsurfa.2017.09.042>
18. Bera, A., Agarwal, J., Shah, M., Shah, S., Vij, R.K.: Recent advances in ionic liquids as alternative to surfactants/chemicals for application in upstream oil industry. *J. Ind. Eng. Chem.* **82**, 17 (2020)
19. Mqoni, N., Singh, S., Bahadur, I., Hashemi, H., Ramjugernath, D.: Ionic liquids, the mixture of ionic liquids and their co-solvent with *N,N*-dimethylformamide as solvents for cellulose using experimental and COSMO study. *Results Eng.* **15**, 100484 (2022). <https://doi.org/10.1016/j.rineng.2022.100484>
20. Negadi, L., Bahadur, I., Masilo, K., Negadi, A.: Excess molar volumes of (2-butoxyethanol or 1-methoxy-2-propanol + benzene or cyclohexane) at (283.15–343.15) K. *Thermochim. Acta* **686**, 178539 (2020). <https://doi.org/10.1016/j.tca.2020.178539>
21. Govinda, V., Reddy, P.M., Bahadur, I., Attri, P., Venkatesu, P., Venkateswarlu, P.: Effect of anion variation on the thermophysical properties of triethylammonium based protic ionic liquids with polar solvent. *Thermochim. Acta*. **556**, 75–88 (2013). <https://doi.org/10.1016/j.tca.2013.02.002>
22. Ali, A., Farooq, U., Uzair, S., Patel, R.: Conductometric and tensiometric studies on the mixed micellar systems of surface-active ionic liquid and cationic surfactants in aqueous medium. *J. Mol. Liq.* **223**, 589–602 (2016). <https://doi.org/10.1016/j.molliq.2016.08.082>
23. Pal, A., Yadav, S.: Effect of a copolymer poly(4-styrenesulfonic acid-co-maleic acid) sodium salt on aggregation behaviour of imidazolium based surface active ionic liquid in aqueous solution. *J. Mol. Liq.* **246**, 342–349 (2017). <https://doi.org/10.1016/j.molliq.2017.09.081>
24. Cheng, N., Ma, X., Sheng, X., Wang, T., Wang, R., Jiao, J., Yu, L.: Aggregation behavior of anionic surface active ionic liquids with double hydrocarbon chains in aqueous solution: experimental and theoretical investigations. *Colloids Surf. Physicochem. Eng. Asp.* **453**, 53–61 (2014). <https://doi.org/10.1016/j.colsurfa.2014.03.083>
25. Kim, M.J., Shin, S.H., Kim, Y.J., Cheong, M., Lee, J.S., Kim, H.S.: Role of Alkyl group in the aromatic extraction using pyridinium-based ionic liquids. *J. Phys. Chem. B* **117**, 14827–14834 (2013). <https://doi.org/10.1021/jp409117j>
26. Kamboj, R., Bharmoria, P., Chauhan, V., Singh, G., Kumar, A., Singh, S., Kang, T.S.: Effect of cationic head group on micellization behavior of new amide-functionalized surface active ionic liquids. *Phys. Chem. Chem. Phys.* **16**, 26040–26050 (2014). <https://doi.org/10.1039/c4cp04054f>
27. Jain, M., Marfatia, A., Imam, N., Ray, D., Aswal, V.K., Patel, N.Y., Raval, V.H., Kailasa, S.K., Malek, N.I.: Ionic liquid-based catanionic vesicles: a de novo system to judiciously improve the solubility, stability and antimicrobial activity of curcumin. *J. Mol. Liq.* **341**, 117396 (2021). <https://doi.org/10.1016/j.molliq.2021.117396>
28. Kaur, R., Kumar, H., Singla, M.: A thermodynamic investigation of the effect of cationic structure on the self-aggregation behavior of surface-active ionic liquids in the presence of an amino acid. *J. Mol. Liq.* **354**, 118904 (2022). <https://doi.org/10.1016/j.molliq.2022.118904>

29. Kumar, H., Kaur, R.: Exploration of the soluting-out effect of carbohydrates on the micellization and surface activity of long-chain imidazolium ionic liquid in the aqueous medium. *J. Mol. Liq.* **319**, 114209 (2020). <https://doi.org/10.1016/J.MOLLIQ.2020.114209>
30. Kaur, G., Kumar, H., Singla, M.: Mixed micellization behavior of 1-dodecyl-3-methylimidazolium chloride [C12mim][Cl] and benzyltrimethyl-*n*-hexadecylammonium chloride (16-BAC) under the influence of gelatin in aqueous media. *J. Mol. Liq.* (2022). <https://doi.org/10.1016/J.MOLLIQ.2022.118479>
31. Chadha, C., Singh, G., Singh, G., Kumar, H., Kang, T.S.: Modulating the mixed micellization of CTAB and an ionic liquid 1-hexadecyl-3-methylimidazolium bromide via varying physical states of ionic liquid. *RSC Adv.* **6**, 38238–38251 (2016). <https://doi.org/10.1039/C6RA05330K>
32. Kumar, H., Kaur, G., Sharma, S.: Investigation of surface adsorption and thermodynamic properties of 1-tetradecyl-3-methylimidazolium bromide in the absence and presence of tetrabutylammonium bromide in aqueous medium. *J. Dispers. Sci. Technol.* (2020). <https://doi.org/10.1080/01932691.2020.1844743>
33. Sharma, R., Mahajan, S., Mahajan, R.K.: Surface adsorption and mixed micelle formation of surface active ionic liquid in cationic surfactants: conductivity, surface tension, fluorescence and NMR studies. *Colloids Surf. Physicochem. Eng. Asp.* **427**, 62–75 (2013). <https://doi.org/10.1016/j.colsurfa.2013.03.023>
34. Mahajan, S., Sharma, R., Mahajan, R.K.: An investigation of drug binding ability of a surface active ionic liquid: micellization, electrochemical, and spectroscopic studies. *Langmuir* **28**, 17238–17246 (2012). <https://doi.org/10.1021/la303193n>
35. Choi, S., Kim, K.S., Lee, H., Oh, J.S., Lee, B.B.: Synthesis and ionic conductivities of lithium-doped morpholinium salts. *Korean J. Chem. Eng.* **22**, 281–284 (2005). <https://doi.org/10.1007/BF02701498>
36. Choi, S., Kim, K., Cha, J., Lee, H., Oh, J.S., Lee, B.: Thermal and electrochemical properties of ionic liquids based on *N*-methyl-*N*-alkyl morpholinium cations. *Korean J. Chem. Eng.* **23**, 795–799 (2006)
37. Rub, M.A., Azum, N., Khan, S.B., Marwani, H.M., Asiri, A.M.: Micellization behavior of amphiphilic drug promazine hydrochloride and sodium dodecyl sulfate mixtures at various temperatures: effect of electrolyte and urea. *J. Mol. Liq.* **212**, 532–543 (2015). <https://doi.org/10.1016/j.molliq.2015.09.049>
38. Azum, N., Ahmed, A., Rub, M.A., Asiri, A.M., Alamery, S.F.: Investigation of aggregation behavior of ibuprofen sodium drug under the influence of gelatin protein and salt. *J. Mol. Liq.* **290**, 111187 (2019). <https://doi.org/10.1016/j.molliq.2019.111187>
39. Ruiz, C.C.: Thermodynamics of micellization of tetradecyltrimethylammonium bromide in ethylene glycol-water binary mixtures. *Colloid Polym. Sci.* **277**, 701–707 (1999). <https://doi.org/10.1007/s003960050443>
40. Shi, L., Li, N., Yan, H., Gao, Y.A., Zheng, L.: Aggregation behavior of long-chain *n*-aryl imidazolium bromide in aqueous solution. *Langmuir* **27**, 1618–1625 (2011). <https://doi.org/10.1021/la104719v>
41. Qin, L., Wang, X.H.: Surface adsorption and thermodynamic properties of mixed system of ionic liquid surfactants with cetyltrimethyl ammonium bromide. *RSC Adv.* **7**, 51426–51435 (2017). <https://doi.org/10.1039/c7ra08915e>
42. Pal, A., Pillania, A.: Modulations in surface and aggregation properties of non-ionic surfactant triton X-45 on addition of ionic liquids in aqueous media. *J. Mol. Liq.* **233**, 243–250 (2017). <https://doi.org/10.1016/j.molliq.2017.03.037>
43. Mahmood, M.E., Al-koofee, D.: Effect of temperature changes on critical micelle concentration for tween series surfactant. *Glob. J. Sci. Front. Res. Chem.* **13**, 1–7 (2013)
44. Kang, K.H., Kim, H.U., Lim, K.H.: Effect of temperature on critical micelle concentration and thermodynamic potentials of micellization of anionic ammonium dodecyl sulfate and cationic octadecyl trimethyl ammonium chloride. *Colloids Surf. Physicochem. Eng. Asp.* **189**, 113–121 (2001). [https://doi.org/10.1016/S0927-7757\(01\)00577-5](https://doi.org/10.1016/S0927-7757(01)00577-5)
45. Alam, M.S., Siddiq, A.M., Mythili, V., Priyadarshini, M., Kamely, N., Mandal, A.B.: Effect of organic additives and temperature on the micellization of cationic surfactant cetyltrimethylammonium chloride: evaluation of thermodynamics. *J. Mol. Liq.* **199**, 511–517 (2014). <https://doi.org/10.1016/j.molliq.2014.09.026>
46. Khan, A.B., Ali, M., Malik, N.A., Ali, A., Patel, R.: Role of 1-methyl-3-octylimidazolium chloride in the micellization behavior of amphiphilic drug amitriptyline hydrochloride. *Colloids Surf. B Biointerfaces.* **112**, 460–465 (2013). <https://doi.org/10.1016/j.colsurfb.2013.08.018>
47. Kumar, H., Kaur, G.: Priya: Influence of tetra ethyl ammonium bromide (C2H5)4NBr on the aggregation behavior of surface active ionic liquid 1-tetradecyl-3-methylimidazolium bromide [C14mim][Br]. *J. Mol. Liq.* (2020). <https://doi.org/10.1016/j.molliq.2020.113431>

48. Singh, T., Kumar, A.: Aggregation behavior of ionic liquids in aqueous solutions: effect of alkyl chain length, cations, and anions. *J. Phys. Chem. B* **111**, 7843–7851 (2007). <https://doi.org/10.1021/jp0726889>
49. Tan, C.H., Huang, Z.J., Huang, X.G.: Rapid determination of surfactant critical micelle concentration in aqueous solutions using fiber-optic refractive index sensing. *Anal. Biochem.* **401**, 144–147 (2010). <https://doi.org/10.1016/j.ab.2010.02.021>
50. Łuczak, J., Łatowska, A., Hupka, J.: Micelle formation of tween 20 nonionic surfactant in imidazolium ionic liquids. *Colloids Surf. Physicochem. Eng. Asp.* **471**, 26–37 (2015). <https://doi.org/10.1016/j.colsurfa.2015.02.008>
51. Shah, M.U.H., Sivapragasam, M., Moniruzzaman, M., Talukder, M.M.R., Yusup, S.B., Goto, M.: Aggregation behavior and antimicrobial activity of a micellar system of binary ionic liquids. *J. Mol. Liq.* **266**, 568–576 (2018). <https://doi.org/10.1016/j.molliq.2018.06.101>
52. Zhang, S., Gao, Y., Dong, B., Zheng, L.: Interaction between the added long-chain ionic liquid 1-dodecyl-3-methylimidazolium tetrafluoroborate and Triton X-100 in aqueous solutions. *Colloids Surf. Physicochem. Eng. Asp.* **372**, 182–189 (2010). <https://doi.org/10.1016/j.colsurfa.2010.10.011>
53. Kumar, D., Rub, M.A., Azum, N., Asiri, A.M.: Mixed micellization study of ibuprofen (sodium salt) and cationic surfactant (conventional as well as gemini). *J. Phys. Org. Chem.* **31**, 1–12 (2018). <https://doi.org/10.1002/poc.3730>
54. Pino, V., Yao, C., Anderson, J.L.: Micellization and interfacial behavior of imidazolium-based ionic liquids in organic solvent-water mixtures. *J. Colloid Interface Sci.* **333**, 548–556 (2009). <https://doi.org/10.1016/j.jcis.2009.02.037>
55. Kumar, D., Azum, N., Rub, M.A., Asiri, A.M.: Aggregation behavior of sodium salt of ibuprofen with conventional and gemini surfactant. *J. Mol. Liq.* **262**, 86–96 (2018). <https://doi.org/10.1016/j.molliq.2018.04.053>

Publisher's Note Springer Nature remains neutral with regard to jurisdictional claims in published maps and institutional affiliations.

Springer Nature or its licensor (e.g. a society or other partner) holds exclusive rights to this article under a publishing agreement with the author(s) or other rightsholder(s); author self-archiving of the accepted manuscript version of this article is solely governed by the terms of such publishing agreement and applicable law.